

# Multifunctional structural supercapacitor composites based on carbon aerogel modified high performance carbon fibre fabrics

*Hui Qian<sup>1,2,3\*</sup>, Anthony R. Kucernak<sup>2</sup>, Emile S. Greenhalgh<sup>1</sup>, Alexander Bismarck<sup>3,4</sup>, Milo S.  
P. Shaffer<sup>1,2\*</sup>*

<sup>1</sup> The Composites Centre, Imperial College London, London, SW7 2AZ, UK;

<sup>2</sup> Department of Chemistry, Imperial College London, London, SW7 2AZ, UK;

<sup>3</sup> Polymer & Composites Engineering (PaCE) group, Department of Chemical Engineering,  
Imperial College London, London, SW7 2AZ, UK;

<sup>4</sup> Institute of Materials Chemistry & Research, PaCE group, Faculty of Chemistry, University  
of Vienna, 1090 Vienna, Austria.

**Keywords:** multifunctional, supercapacitors, carbon fibre, carbon aerogel, composites

---

\* Corresponding authors. E-mail addresses: [m.shaffer@Imperial.ac.uk](mailto:m.shaffer@Imperial.ac.uk) (M. Shaffer); [hui.qian@imperial.ac.uk](mailto:hui.qian@imperial.ac.uk) (H. Qian)

**Abstract:**

A novel multifunctional material has been designed to provide excellent mechanical properties whilst possessing a high electrochemical surface area suitable for electrochemical energy storage: structural carbon fibre fabrics are embedded in a continuous network of carbon aerogel (CAG) to form a coherent but porous monolith. The CAG-modification process was found to be scalable and to be compatible with a range of carbon fibre fabrics with different surface properties. The incorporation of CAG significantly increased the surface area of carbon fibre fabrics, and hence the electrochemical performance, by around 100-fold, resulting in a CAG-normalised specific electrode capacitance of around  $62 \text{ Fg}^{-1}$ , determined by cyclic voltammetry in an aqueous electrolyte. Using an ionic liquid (IL) electrolyte, the estimated energy density increased from  $0.003$  to  $1 \text{ Whkg}^{-1}$ , after introducing the CAG into the carbon fibre fabric. ‘Proof-of-concept’ multifunctional structural supercapacitor devices were fabricated using an IL-modified solid-state polymer electrolyte as a multifunctional matrix to provide both ionic transport and physical support for the primary fibres. Two CAG-impregnated carbon fabrics were sandwiched around an insulating separator to form a functioning structural electrochemical double layer capacitor composite. The CAG-modification not only improved the electrochemical surface area, but also reinforced the polymer matrix surrounding the primary fibres, leading to dramatic improvements in the matrix-dominated composite properties. Increases in in-plane shear strength and modulus, of up to 4.5-fold, were observed, demonstrating that CAG-modified structural carbon fibre fabrics have promise in both pure structural and multifunctional energy storage applications.

## 1. Introduction

Multifunctional materials are specifically developed to improve system performance and efficiency by reducing redundancy between subsystem components and functions.<sup>1</sup> The combination of structural and electrochemical energy storage/power functions in a single material, to provide multifunctional structural energy storage/power devices,<sup>2</sup> offers the opportunity to significantly reduce the weight and volume of mobile systems that currently rely on traditional, independent energy storage devices and load-carrying structural materials. Such systems are relevant to a wide range of applications, particularly in aerospace, electric/hybrid ground transport and portable electronics, where battery life and power management are limiting issues. In particular, radical new approaches to energy storage are required to progress towards future zero emission electrical vehicles.<sup>3</sup>

To date, two main strategies have been applied to the fabrication of multifunctional structural energy storage devices. One straight-forward approach is a *multifunctional structure*, physically embedding energy storage devices into conventional fibre-reinforced composites<sup>4</sup> or using structural composite laminates as packaging to protect the devices.<sup>5</sup> Such devices have been reported to operate normally under low mechanical loads. However, this approach offers only modest mass/volume savings and issues such as delamination at the device/composite interface may be limiting. An alternative potentially more beneficial route is to produce truly *multifunctional materials*, consisting of multifunctional composite constituents that simultaneously and synergistically provide structural and electrochemical energy storage functions.<sup>6</sup> Earlier work has been focused on multifunctional structural batteries<sup>7</sup> and dielectric capacitors<sup>8</sup>. The concept developed in this work is that of multifunctional structural supercapacitor composites, initially focusing specifically on electrical double layer capacitors (EDLCs), but with an obvious possible extension to pseudocapacitor devices, incorporating redox active elements.<sup>9</sup> Supercapacitors are attracting increasing interest due to their high power density, long cycle life, and good reversibility

compared to batteries and high energy density compared to dielectric capacitors.<sup>9-10</sup> They are particularly interesting in the context of multifunctional energy storage devices because they offer relatively high energy density, by internal redistribution of electrons and electrolyte ions; by avoiding the physical dissolution or deposition of electrode materials associated with batteries, it is simpler to maintain structural integrity. Flexible supercapacitors have been developed previously to maintain mechanical integrity during packaging,<sup>11</sup> and for integration with smart textiles.<sup>12</sup> The goal, here, is to develop strong, stiff, multifunctional supercapacitors, capable of full structural function, ultimately akin to a normal fibre-reinforced polymer composites.

This work was initially motivated by a recognition that carbon-based materials are often used both for electrochemical devices, and high performance structural composites; in addition, both electrochemical devices and structural fibre-reinforced polymer composites are usually assembled in a laminated form. Thus, the goal was to produce a multifunctional structural supercapacitor built around laminated structural carbon fibre fabrics. As shown in **Scheme 1**, each cell of the proposed structural supercapacitor consists of two modified structural carbon fibre fabric electrodes, separated by a structural glass fibre fabric or polymer membrane, infused with a multifunctional polymeric electrolyte.<sup>6a</sup> There are two crucial components: one is an electrolyte that both allows ionic motion and provides adequate mechanical support, interfacial adhesion, and cohesion; the other is a multifunctional electrode that possesses high energy storage capability and good mechanical performance. Preliminary work based on as-received structural carbon fibre fabrics (details are included in the results and discussion section) demonstrated the feasibility of the multifunctional material concept, but with very low energy storage capability. The poor performance was mainly due to the intrinsic low surface area ( $< 1 \text{ m}^2\text{g}^{-1}$ ) of structural carbon fibres that are suitable for high performance mechanical reinforcement (e.g. with tensile strength  $>3000 \text{ MPa}$ ). It is well known that the

energy storage capability of EDLCs directly depends on the specific surface area of the electrodes.<sup>13</sup> High surface area, carbon-based materials, including a variety of activated carbons, are typically used as electrodes for traditional EDLCs.<sup>9, 14</sup> However, activated carbon fibre fabrics are never fully graphitised and have only very poor mechanical performance: tensile strengths are only a few tens of MPa, and thus are not suitable for mechanical reinforcement of multifunctional structural electrodes.

A fundamental challenge, in the current context, is to improve the electrochemical properties of structural carbon fibres by increasing their surface area, without degrading their mechanical performance. Different strategies have been investigated in our Group, including both chemical activation<sup>15</sup> and carbon nanotube grafting.<sup>16</sup> Considerable improvements have been observed in specific surface area. However, these methods involve etching of the carbon fibre surface by either the activating chemicals or the catalyst for growing carbon nanotubes; process parameters need to be carefully controlled to avoid degradation of the fibre mechanical properties and the total volume available for the active material is limited. Here, we consider a different, non-damaging modification route that involves embedding structural carbon fibres into a monolithic carbon aerogel (CAG) structure. As one type of conventional electrode for EDLCs, CAGs are unique porous materials<sup>17</sup> consisting of a three dimensional network of interconnected nanometre-sized particles with small interstitial pores, leading to typical surface areas of 400-1100 m<sup>2</sup>g<sup>-1</sup>. Thin sheets of monolithic CAGs normally have poor mechanical stability and handlability. Embedding carbon paper/felt consisting of non-structural discontinuous carbon fibres into CAGs has been shown previously to ease processing for conventional EDLCs, whilst simultaneously improving the electrical conductivity of the electrodes,<sup>18</sup> However, these materials are not suitable for structural supercapacitor applications due to the relatively poor mechanical properties of the non-structural carbon papers. Here, by combining structural carbon fibres with high surface area

CAGs, the resulting materials can both provide high energy storage capacity, and also serve as the mechanical reinforcement in the multifunctional composite structure. In addition, the CAG surrounds the fibres and extends into the polymer electrolyte/matrix; this aspect may be extremely helpful for overcoming the other main challenge of the multifunctional supercapacitors: achieving high ionic conductivity without critically reducing the mechanical performance of the polymer electrolyte/matrix.

This paper presents a ‘proof-of-concept’ study of multifunctional structural supercapacitors based on high performance structural carbon fibre fabrics. A multifunctional electrode material is developed by infusing CAGs into low-weight structural (high mechanical performance) carbon fibre fabrics (Scheme 1). Different fabrication methods are compared and the effects on the resulting surface morphology and electrochemical properties are reported. Structural supercapacitors were manufactured using scaled-up, optimised conditions: assessments of both electrochemical and mechanical performance of these devices are provided, together with a discussion of the prospects for this new form of multifunctional energy storage device.

## **2. Experimental section**

### **2.1. Materials and chemicals**

HTA 3k plain weave carbon fibre fabrics ( $200 \text{ gm}^{-2}$ , TISSA Glasweberei AG) were used for the electrode materials. Two separator materials were used: a glass fibre fabric (plain weave,  $200 \text{ gm}^{-2}$ , 842.0200.01, TISSA Glasweberei AG) and polypropylene membrane (PP, monolayer 3500, surface treated to be hydrophilic, Celgard). All chemical reagents were purchased from Sigma-Aldrich, and were used as-received. T300 3k 5-satin-harness weave carbon fibre fabrics ( $283 \text{ gm}^{-2}$ , ACG) and chemically-activated HTA carbon fibre fabrics (see fabrication details in reference<sup>15a, b</sup>) were used to study the universality of the CAG-impregnation process.

### **2.2. Fabrication of CAG-modified carbon fibre fabrics**

Resorcinol-formaldehyde (RF) polymer was prepared using the commercially-available RF resin (AX2000, INDSPEC Chemical Corporation). The AX-2000 resin contains about 73.1 wt.% resorcinol, at a R:F molar ratio of 2:1. Potassium hydroxide (KOH) was used as the catalyst (C) and the R:C molar ratio was 50:1. Extra formaldehyde (37 wt.% solution) was added to the mixture to keep the R:F ratio at 1:2. The weight percentage of the RF in mixture was controlled to be 40% by adjusting the quantity of the diluent distilled water. The mixture was tightly sealed and stirred for 2 h. Two different methods were applied to coat carbon fibre fabrics with RF: (1) Pressing route: carbon fibre fabrics were soaked in RF solution for 2 h and then pressed between two clean glass microscope slides (102x152 mm, 1.2-1.5 mm, Logitech Ltd.), which were clamped on both ends to form a thin film of RF coating the carbon fibre fabrics. The pressed sample was then taped and wrapped in aluminium foil and placed in air-tight box to retard evaporation. (2) Infusion route: RF solution was infused into the carbon fibre fabrics with a version of the Resin Infusion under Flexible Tooling (RIFT) method often used for fibre-reinforced polymer composite fabrication (see below 'Fabrication of structural supercapacitors' for details). Specimens prepared using different methods were cured at room temperature, 50°C and 90°C with a period of 24 h at each temperature. The dried specimens were then carbonised at 800°C for 30 min in a furnace (Lenton ECF 12/30) under N<sub>2</sub>, flowing at 0.5 L min<sup>-1</sup>.

### **2.3. Morphology and surface characterisation of CAG-modified carbon fibre fabrics**

The microstructure of the carbon fibre fabrics was characterised using a field emission gun scanning electron microscopy (SEM) (Gemini LEO 1525 FEG-SEM, Carl Zeiss NTS GmbH), operating at 5 kV, without metal coating. Specific surface area and pore size of the CAG-modified carbon fibre fabrics were studied using a Micromeritics TriStar 3000 analyser (Micromeritics UK Ltd.) with pure N<sub>2</sub>, based on the Brunauer, Emmet, Teller (BET) and the Barrett, Joyner and Halenda (BJH) methods.

### **2.4. Electrochemical characterisation of CAG-modified carbon fibre fabrics**

Electrochemical tests were performed on the carbon fibre fabric tows (3k fibre bundles, around 3.5 cm long) before and after the CAG coating process at ambient temperature, using a three-electrode cell (platinum wire counter electrode, silver-silver chloride (Ag/AgCl) reference electrode and 3 M KCl aqueous solution (Sigma-Aldrich)). CV experiments were conducted between -0.2 and +0.2 V, at different scan rates ranged from 1 to 100 mVs<sup>-1</sup>, using a SI 1287 electrochemical interface (Solartron Instruments). The scan range (potential window) of -0.2 V to 0.2 V was chosen for this work as it provided representative capacitance results and allowed for quick comparison between different specimens. Wider potential windows up to ±1 V were tested and consistent capacitance values were obtained (Figure S1).

## **2.5. Fabrication of structural supercapacitors**

Three different matrix systems were compared: conventional structural diglycidylether of bisphenol-A (DGEBA)-based epoxy, polyethylene glycol diglycidyl ether (PEGDGE,  $M_n \sim 526$ )-based epoxy, and a multifunctional polymer electrolyte based on the PEGDGE system. Tri-ethylene-tetramine (TETA, molar ratio of PEGDGE:TETA $\sim$ 3:1) and 4,4'-diamino dicyclohexyl methane (PACM, molar ratio of DGEBA:PACM $\sim$ 2.3:1) were used as the crosslinkers for PEGDGE and DGEBA, respectively. To produce a multifunctional electrolyte matrix, 10 wt.% ionic liquid, 1-ethyl-3-methylimidazolium bis(trifluoromethylsulfonyl) imide (EMITFSI, purity  $\geq$  98%), was mixed into PEGDGE (82.6 wt.%), with a stirrer bar, until a homogeneous solution was obtained. TETA (7.4 wt.%) was then added to the solution. All resin mixtures were degassed before infusion using the RIFT method. RIFT can be considered as a variant on resin transfer moulding (RTM) in which one tool face is replaced by a flexible film allowing for more flexibility in the geometry of the laminate.<sup>19</sup> The layup for producing structural supercapacitors consisted of two carbon fabric electrodes, which sandwiched two glass fabrics as the separator (mirrored



at the mid-plane to ensure the laminates were symmetrical, for mechanical testing). Copper tape (with conductive adhesive, 542-5511, RS components) was applied to the carbon fibre fabrics, to form the current collector for electrochemical characterisation. The resin was then infused under 1 bar into the vacuum bag containing the fabrics. The curing of PEGDGE-based and DGEBA-based specimens was performed at 80°C for 24 h and at room temperature for 48 h, respectively.

## 2.6. Electrochemical characterisation of structural supercapacitors

The dimensions of the supercapacitors were around 6.5×7.5 cm. Charge-discharge experiments were performed at room temperature using a SI 1287 electrochemical interface (Solartron Instruments) with a 0.1 V step voltage applied for 60 s. Electrical characteristics were evaluated based on a simplified electrical equivalent circuit of the system (Figure 4c). In this model, charge is stored in a capacitor of capacitance of  $C_{SP}$ .  $R_p$  is the parallel resistance that characterises any electrical contact between the two electrodes or electrochemical reactions.  $R_s$  (ESR) is the sum of the electrical resistance of the electrodes and the ionic resistance of the electrolyte between these electrodes. The capacitance,  $C_{SP}$ , and resistances,  $R_s$  and  $R_p$ , were determined by fitting the charge transient responses to the current-time response of the equivalent circuit<sup>20</sup> (Figure 4d):

$$I(t) = \frac{U_{applied}}{R_s} e^{-\frac{t}{\tau}} + \frac{U_{applied}}{R_s + R_p} \left( 1 - e^{-\frac{t}{\tau}} \right) \quad \text{Equation 1}$$

where  $R_s$ ,  $R_p$ , and  $\tau$  were the fitting parameters. The capacitance was determined from:

$$C_{SP} = \frac{\tau(R_s + R_p)}{R_s R_p} \quad \text{Equation 2}$$

The power and energy densities of the systems were calculated from:<sup>21</sup>

$$E = \frac{1}{2} C_{SP} U_{applied}^2 \quad \text{Equation 3}$$

$$P = \frac{U_{\text{applied}}^2}{4R_s}$$

Equation 4

## 2.7. Mechanical characterisation of structural supercapacitors

The in-plane shear properties of the structural supercapacitors were investigated by tensile testing of a  $\pm 45^\circ$  laminate according to the ASTM standard<sup>22</sup> D3518. The alignment of the carbon fabric plies was checked before and after the CAG fabrication process. The composite specimens prepared using RIFT were cut to dimensions of 150×25 mm. Glass-fibre composite end-tabs were then applied to both ends of each specimen, resulting in a gauge length of 90 mm. A biaxial strain gauge (FCA-5-11, Techni Measure) was adhered to the sample using cyanoacrylate glue at the mid-span of the specimens to measure the strains in both the longitudinal and transverse directions. The tests were conducted at room temperature using an INSTRON 4505 universal testing machine, equipped with a 10 kN (for DGEBA-based specimens) or 1 kN (for PEGDGE-based specimens) load cell, with a crosshead speed of 2 mm min<sup>-1</sup>. A minimum of five measurements were conducted for each type of specimen. The fibre volume fraction of the reinforcements in the composites was measured according to the standard<sup>23</sup> ASTM D3171 Method II, based on calculations using areal weight of reinforcement.

## 3. Results and discussion

### 3.1. Fabrication and characterisation of CAG-modified carbon fibre fabrics

#### 3.1.1. Comparison of different fabrication routes of CAG-modified carbon fibre fabrics

CAGs can be fabricated from a wide range of organic precursor gels,<sup>24</sup> among which resorcinol-formaldehyde (RF) is the most widely used. A commercially available RF resin (kindly supplied by Indspec Chemical Co.), which contained oligomers formed by pre-mixing RF in a certain proportion, was used in this work in order to shorten the RF gelation time. The formation of RF gels was based on the sol-gel polycondensation mechanism and the organic gels were then converted into CAGs through a carbonisation step under an inert

environment.<sup>25</sup> Two different methods were used to fabricate CAG-modified carbon fibre fabrics. The ‘pressing route’, involving pressing the RF sol-soaked carbon fibre fabrics between two glass slides, has been used previously for the fabrication of carbon fibre paper-reinforced CAGs,<sup>18b, 26</sup> containing up to 94 wt.% CAG. However, in order to utilise the excellent mechanical properties of carbon fibres in a multifunctional composite structure, a high loading fraction of carbon fibres is needed; around 55-60 vol.% is typical for woven structural composites.<sup>27</sup> For this reason, an alternative infusion route was developed, to provide thin, uniform laminates of CAG-modified carbon fibre fabrics. Vacuum-assisted infusion methods have been widely used for resin infusion in traditional fibre-reinforced composite manufacturing,<sup>19</sup> highlighting their suitability for large-scale manufacturing. In addition, compared to simple pressing, the vacuum-assisted infusion process applies greater and more uniform pressure on the carbon fibre fabrics, which should be more suitable for a dense, high fibre-loading composite. By keeping the CAG layer thin, electrolyte penetration and ion diffusion should be easier, improving the electrochemical,<sup>14</sup> as well as mechanical performance, of the ultimate multifunctional composite. In line with this expectation, a lower CAG loading (15.9 wt.%) was observed for the infused specimens compared to that of the pressed specimens (22 wt.%). The loading of CAG is much lower in both cases, than for previous work using carbon felts/papers,<sup>18</sup> due to the more compact arrangement of aligned fibres in the structural weaves. SEM observations show the typical surface crenulations of as-received structural carbon fibres (Fig. 1a), which form during the fibre manufacturing process. After the CAG-modification, a relative uniform coating of CAGs was successfully formed on the fibre surfaces (Fig. 1b). The gaps between carbon fibres within the fibre bundles were also successfully filled with nanostructured CAGs (Figure 1c), which themselves possessed an interconnected pore structure with interstitial pores of a few tens of nanometres, as clearly seen in the close-up image (Figure 1d), creating a hierarchical

reinforcement structure. However, due to the low pressure applied during the pressing route, CAG-rich regions were formed on both faces of the carbon fibre fabrics, which would introduce undesirable resin-rich regions in the subsequent composite fabrication process and reduce the mechanical performance, particularly in bending. In contrast, the high pressure applied using the RIFTing method effectively reduces the formation of resin-rich regions and improves mechanical properties.

Very significant increases in specific surface area were achieved by modifying carbon fibre fabrics with porous CAGs (Table 1). The improvements were consistent with the CAG loading, implying similar CAG-normalised specific surface area (around  $740 \text{ m}^2\text{g}^{-1}$ ) for specimens prepared using different methods; this typical CAG-normalised surface area is comparable to that reported in literature<sup>28</sup>, in the range of  $400\text{-}900 \text{ m}^2\text{g}^{-1}$ . However, the shrinkage of the CAG network was constrained by the embedded carbon fibre fabrics, leading to lower density and higher surface area, as compared to the pure CAG structure fabricated under similar conditions. An equivalent phenomenon was reported, previously, for non-woven carbon fibre-embedded CAGs.<sup>18a</sup> Significant increases in pore volume were observed after CAG modification (Figure 2). Both of the CAG-modified specimens showed type IV curves according to the IUPAC classification,<sup>29</sup> exhibiting hysteresis loops between the adsorption and desorption isotherms, typical of mesoporous CAG specimens.<sup>30</sup>

The electrochemical properties of the structural carbon fibre fabrics were studied using cyclic voltammetry (CV) (Figure 3a), before and after CAG-modification, using a conventional electrolyte (3 M KCl aqueous solution). Specific current densities were converted to specific capacitances by dividing by the scan rate. For both fabrication methods, a relatively symmetric and rectangular shape was observed, associated with pure capacitive behaviour. No redox peaks were observed, as expected, for annealed carbon-based materials.<sup>31</sup> The specific capacitances derived from the CV measurements (Table 1) showed very large

improvements on introducing CAG into carbon fibre fabrics, with a greater effect for the pressed CAG-modified fabrics due to the higher CAG loading. Wider potential windows (up to -1 to 1 V) were tested and consistent capacitance values were observed (Figure S1). Figure 3b shows the specific capacitance obtained from the cyclic voltammograms (shown inset) as a function of scan rate. A rectangular shape characteristic of capacitive behaviour is preserved across a range of scan rates up to  $100 \text{ mVs}^{-1}$ . The specific capacitance decreases with increasing scan rate as typically seen with carbon-based double layer electrodes, due to recognised phenomena associated with ionic resistance, micropore blocking, or ion depletion.<sup>18a, 32</sup>

### *3.1.2. Scaling-up of the fabrication process of CAG-modified carbon fibre fabrics*

Based on these preliminary successes, the infusion process was then scaled-up: CAG-modified carbon fibre fabrics with dimensions of 22x17 cm were successfully fabricated. The maximum size of the scaled-up laminates was dictated by the active area of the chamber furnace used in the carbonisation process, rather than a fundamental limit. As shown in Table 1, a typical CAG-loading around 9 wt.% was obtained, slightly lower than that for the small specimens fabricated using the same method. This reduction is attributed to the use of a less viscous RF sol for the scaled-up process, to prevent gelation during infusion (viscosity is reduced simply by stirring the RF sol for a shorter period before use). The consistency of the specific capacitance normalised to the CAG-loading (around  $62 \text{ Fg}^{-1}$ ), shows that the scale-up did not significantly affect the electrochemical properties of the CAG. In addition, the same fabrication process was applied to other types of structural carbon fibre fabrics with different surface chemistries and morphologies, including chemically-activated HTA carbon fibre fabrics with a rough surface structure<sup>15a, b</sup> and T300 carbon fibre fabrics with different sizing and weaving styles. Improvements in surface area and electrochemical performance were observed regardless of the fibre type and their surface properties (Supporting information,

Table S1 and Figure S2), suggesting a wide applicability of the fabrication process for CAG-modified structural carbon fibre fabrics.

### 3.2. Electrochemical characterisation of structural supercapacitors

Ionic liquids (IL) are very interesting electrolytes for energy storage applications due to their unique physicochemical properties<sup>33</sup>, including high thermal and hydrolytic stability, negligible vapour pressure, relatively high ionic conductivity, and large electrochemical windows (up to 7 V). Higher operating voltage boosts both the energy and power density, which are both proportional to the square of the applied voltage.<sup>10</sup> The electrochemical properties of supercapacitors based on CAG-modified carbon fabric electrodes were initially investigated in IL using charge-discharge measurements (Figure 4a), demonstrating consistent improvements (over 100-fold) in specific capacitance independently of the separator configurations (Table 2). These results suggest good accessibility of the IL into the porous CAG structure to achieve a high EDL capacitance. In addition, the CAG-based supercapacitors exhibited a lower equivalent series resistance (ESR,  $R_s$ ) than the bare carbon fibre control devices, dropping from around 40 to 0.2  $\text{k}\Omega\text{cm}^2$ . ESR depends on a number of factors including the active area, porosity, and electrical resistance of the electrodes, as well as the ionic resistance of the electrolyte, and any interfacial resistance between the electrolyte and electrode.<sup>34</sup> The improvement observed on CAG modification may be associated with improved transverse conductivity between the primary carbon fibres, and a reduction in the interfacial resistance between carbon surface and electrolyte (since the fibres are sized initially). The energy and power densities, calculated using the applied voltage of 0.1 V showed improvements by a factor of around 200 after the CAG modification. With the use of IL as electrolyte, under dry conditions, the voltage window can be expanded in future; an estimation of the energy and power densities of CAG-modified specimens based on a working voltage of 3 V would reach around 1  $\text{Whkg}^{-1}$  and 0.3  $\text{kWkg}^{-1}$ , respectively, which

begins to approach typical values<sup>35</sup> of traditional supercapacitors, 5 Wh kg<sup>-1</sup> and 0.2-10 kW kg<sup>-1</sup>.

For multifunctional supercapacitor devices, a multifunctional solid-state electrolyte is required that both supports ion conduction and can ensure mechanical load transfer between the reinforcing fibres. Polymer electrolytes are attractive in pure electrochemical devices because they offer flexible, compact, laminated solid-state structures free from leaks and are available in different geometries.<sup>36</sup> Poly(ethylene oxide) (PEO) is a common choice as a polymer network which can entrap up to 80 wt.% organic solvent and reach ionic conductivities<sup>37</sup> on the order of 10<sup>-3</sup> Scm<sup>-1</sup>. However, the poor mechanical stability of PEO limits its application as a multifunctional structural polymer electrolyte/matrix. In this work, an IL-modified epoxy matrix based on PEGDGE, crosslinked with amine-based crosslinker, was used as a solid-state polymer electrolyte for fabricating ‘proof-of-concept’ structural supercapacitors. The PEGDGE-based epoxy resin has modest mechanical properties (Young’s modulus<sup>38</sup> of around 6 MPa) compared to traditional structural epoxy resins (such as bisphenol-A based epoxy with a Young’s modulus of around 3 GPa), but offers reasonable ionic conductivity.<sup>39</sup> As shown in Table 2, the specific capacitances determined via fitting the charge-discharge responses (Figure 4b) showed improvements in the CAG-modified structural supercapacitors, but the increases were lower than those obtained in aqueous electrolyte (3M KCl solution) or pure IL. The reduced capacitance and increased ESR of the CAG-devices based on polymeric electrolyte resulted in a considerable decrease of both the energy and power density, which were much lower compared to typical values for traditional monofunctional or flexible supercapacitors. The limitation can be mainly attributed to the reduced ionic conductivity of the polymeric electrolyte, from around 9 mScm<sup>-1</sup> for pure IL to 2.8×10<sup>-2</sup> mScm<sup>-1</sup> for PEGDGE epoxy mixed with 10 wt.% IL, resulting in a significantly increased ESR and considerably longer charging/discharging timescale. The as-received CF

PEDGE system still has a high ESR probably dominated by interface effects, rather than bulk ionic conductivity (a slight improvement may be associated with partial dissolution of the size into the resin)..

Different separator materials, including structural glass fabrics and polymer membranes, were used for assembling supercapacitors and their effects on the electrochemical properties of the devices were investigated. Polypropylene (PP) membranes are widely used in battery industry and have low thickness (25  $\mu\text{m}$ ) and high porosity (~55%). However, their poor mechanical properties and the tendency to promote delamination in the composites make them less ideal than glass fibre (GF) fabrics as separators in multifunctional structural supercapacitors. The thickness of GF used in this work was around 160  $\mu\text{m}$ , because the commercially available, lighter fabrics were not sufficiently dense to prevent short-circuiting. Low specific weight glass fabrics tend to have 'windows' in the weave rather than reduced thickness. Devices containing two pieces of GF were also assembled for consistency with the 'balanced' configuration required for mechanical characterisation (see below). On the other hand, the GF limits the performance of the CAG devices with the PEDGE matrix, since, in these cases, the bulk ionic resistance dominates the ESR. As expected, the resistance effects are more pronounced for the thicker GF separator, than the thinner commercial PP membrane.

### **3.3. Mechanical characterisation of structural supercapacitors**

The fibre-dominated behaviour of composites based on CAG-modified carbon fabrics can be expected to retain the excellent properties of the underlying structural weave; for example, tensile strengths and stiffness, which are dominated by the fibre performance, should be unaffected.<sup>27</sup> However, a much more critical, and demanding question is whether the matrix-dominated properties, which typically limit overall composite component design, are adversely affected by the poor mechanical performance of the multifunctional matrix. On the other hand, the presence of the stiff CAG network offers an intriguing means to improve the effective matrix properties, and to provide additional support to the fibres. For these reasons,



the mechanical testing effort was focussed on the assessment of in-plane shear properties, in order to probe the influence of the new CAG modified matrix and fibre/matrix interface on composite performance. In addition, the format of the shear specimens allowed simultaneous testing of electrochemical properties, without requiring large amounts of material. Clearly, this single test method does not provide a comprehensive mechanical characterisation, but it does focus on the most diagnostic property with which to evaluate the multifunctional matrix materials developed. Further studies, considering a wide spectrum of conventional tests, including longitudinal compression and interlaminar shear are under way. In the current shear tests, three different matrix systems were compared, including conventional structural bisphenol-A (DGEBA)-based epoxy, PEGDGE-based epoxy, and multifunctional polymer electrolyte (cross-linked PEGDGE containing 10 wt.% IL). All the specimens were stiff, structurally robust and possessed good handlability. Typical shear stress–strain curves are shown in Figure 5. Higher loads were recorded in the case of DGEBA-based composites, as expected, leading to higher shear strength compared to the other two PEGDGE-based systems. The shear stress increased linearly up to around 3000 microstrain, from this range the shear modulus was calculated. The failure of all specimens involved damage accumulation in the matrix followed by delamination between the carbon and glass layers (Figure S3a, b); similar failure mechanisms for woven carbon fibre/polymer structural composites are reported in the literature.<sup>41</sup> As summarised in Table 3, the shear modulus of the DGEBA-based composites increased by around 15% due to the stiffening effect of the CAG-modification, whilst the shear strength remained constant. For the PEGDGE-based specimens, the presence of the CAGs improved the shear properties of the composite significantly, with a 4.5-fold and 1.6-fold improvement in shear modulus and shear strength, respectively; filling the CAG pores with IL had no further effect. The fractographic study<sup>42</sup> showed similar fracture morphologies for the baseline and CAG-modified specimens,

including both matrix plasticity and ductile fracture (Figure S3c, d), indicating good infusion/penetration of the epoxy matrix into the CAG porous structure. In addition, good adhesion between the fibres and the matrix was observed. One of the major limitations in the practical application of conventional fibre-reinforced composites is the relatively poor performance in matrix-dominated properties (for example, in-plane and interlaminar shear strengths).<sup>43</sup> Extensive attempts have been made to improve the matrix-dominated properties by introducing nanoparticles,<sup>44</sup> carbon nanotubes,<sup>45</sup> or rubber phases<sup>46</sup> into the polymer matrix, or by creating hierarchically-reinforced composites.<sup>45</sup> In the current case, the CAG could be considered to be a nanoreinforcement in a hierarchical composite structure, with enhanced matrix-dominated properties. This unexpected benefit of CAGs on the mechanical performance of conventional polymer composites is novel and suggests a route towards the future development of both multifunctional structural energy storage devices and conventional structural composites. In the former case, the relatively soft/weak polymer electrolyte formulations (required for good ionic conductivity) can be augmented by the stiff CAG microstructure, leading to both good structural and electrochemical performance. The results reported here show that CAG-modification not only improves the specific capacitance of the carbon fibre weave electrodes, but also reinforces the IL-modified polymer electrolyte.

#### **4. Conclusions and outlook**

The creation of multifunctional structural energy storage materials offers mass/volume savings in many applications that currently rely on independent energy storage devices and inert structural components. The structural supercapacitor is a compelling embodiment as it is simpler to maintain structural integrity whilst offering useful energy performance, compared to other energy storage systems, such as structural batteries. It is also important to note that the individual functionalities of multifunctional structural supercapacitors do not need to achieve state-of-the-art performance of conventional monofunctional supercapacitors or fibre-reinforced structural polymer composites. The synergy of having a single

multifunctional material that undertakes multiple tasks simultaneously allows for some compromise in the individual properties.<sup>47</sup> The benefits of saving mass system and improving energy efficiency can still be obtained with an appropriate balance of the two functions.

This paper successfully demonstrates successful structural supercapacitors, where the mechanical performance is not simply a matter of robustness, as in the case of flexible supercapacitors<sup>11</sup>, but based on a genuine high strength, high stiffness structural fibre composite. The development of new CAG-modified, structural carbon fibre fabrics provides one of the two critical multifunctional constituents required to realise this ambition. Pure electrochemical testing demonstrated the suitability of these nanostructures reinforcements as high surface area electrode materials based on a range of structural carbon fibres. Relatively large samples were then successfully fabricated using resin infusion, an approach suitable for large-scale manufacturing. After carbonisation, the porous reinforcement/electrodes were combined with a structural insulating spacer and impregnated with a multifunctional matrix/electrolyte. These structural supercapacitor composites exhibited excellent mechanical characteristics; the use of IL-modified polymeric electrolytes clearly demonstrated effective storage of electrical energy through EDL capacitance. However, the power and energy densities obtained using the polymeric electrolyte matrix were much lower than those obtained with aqueous electrolyte or pure IL. Whilst the CAG-modified carbon fibre system provides an excellent multifunctional reinforcement, the second major challenge, of a multifunctional electrolyte needs further development. The current PEG-based system is limited by the ionic conductivity of the polymeric matrix/electrolyte, the electrode/electrolyte interface, and the thickness of the structural separator. A multifunctional polymeric electrolyte/matrix that provides good electrochemical and mechanical characteristics is the other key constituent for a successful structural supercapacitor. Providing both properties is a challenge because increasing the rigidity of the polymer structure tends to interrupt ion

transport and depress ionic conductivity.<sup>48</sup> Interestingly, the CAG-based structure may help to resolve these opposing tendencies, by providing rigidity between the primary fibres. Indeed, filling the CAG pore volume with pure IL illustrates one potential limiting case with relatively good performance, if an appropriate separator is used. To improve the current polymer electrolyte/matrix further, the IL concentration must be optimised with a suitable polymer (nanostructure); the introduction of copolymer,<sup>49</sup> gel crosslinked with structural matrix,<sup>37</sup> or organic-inorganic hybrid electrolyte<sup>50</sup> all offer possible solutions. Further improvements in energy and power densities can, therefore, be anticipated on optimisation of the solid-state electrolyte/matrix, in the future.

Finally, it is worth noting that the continuous CAGs can serve as a matrix nanoreinforcement in traditional fibre-reinforced structural composites to form a hierarchically reinforced structure that may enhance pure mechanical performance. The CAG monolith distributed around the carbon fibres can be expected to stiffen the surrounding matrix, similar to the usage of carbon nanotubes grafted onto carbon fibres,<sup>16, 45, 51</sup>. The CAG may thus support the fibres against microbuckling, which is the critical composite failure mode associated with fibres under longitudinal compression, as well as modifying matrix toughness. Further studies of pure structural systems are warranted.

### **Supporting Information**

Supporting Information Available: Surface properties (Table S1 and Figure S2) of CAG-modified chemically-activated HTA and T300 carbon fibres. CV measurements of CAG-modified carbon fibres at different potential windows (Figure S1). Photos and SEM images of tested composite specimens (Figure S3). This material is available free of charge via the Internet at <http://pubs.acs.org>.

### **Acknowledgements**

This work is funded by EU Seventh Framework Programme Theme 7 StorAGE (No. 234236).

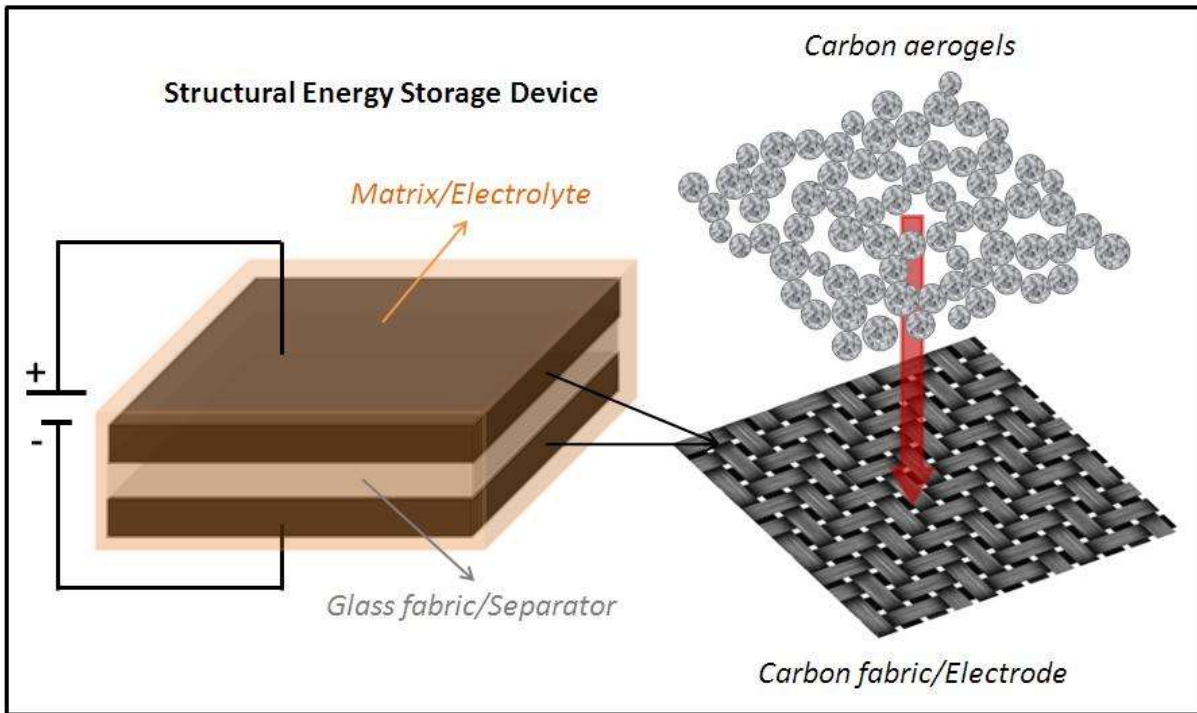
## References

1. Christodoulou, L.; Venables, J., *J. Min. Metals Mater. Soc.* **2003**, *55*, 39-45.
2. Gibson, R. F., *Compos. Struct.* **2010**, *92*, 2793-2810.
3. Karden, E.; Ploumen, S.; Fricke, B.; Miller, T.; Snyder, K., *J. Power Sources* **2007**, *168*, 2-11.
4. Pereira, T.; Guo, Z.; Nieh, S.; Arias, J.; Hahn, H. T., *Compos. Sci. Technol.* **2008**, *68*, 1935-1941.
5. Thomas, J.; Qidwai, M., *J. Min. Metals Mater. Soc.* **2005**, *57*, 18-24.
6. (a) Shaffer, M.; Greenhalgh, E.; Bismarck, A.; Curtis, P. **2007**, **WO/2007/125282**; (b) Snyder, J. F.; O'Brien, D. J.; Baechle, D. M.; Mattson, D. E.; Wetzel, E. D. Proceedings of the ASME Conference on Smart Materials, Adaptive Structures and Intelligent Systems, 2008; pp 1-8.
7. (a) Liu, P.; Sherman, E.; Jacobsen, A., *J. Power Sources* **2009**, *189*, 646-650; (b) Snyder, J. F.; Carter, R. H.; Wong, E. L.; Nguyen, P. A.; Xu, K.; Ngo, E. H.; Wetzel, E. D. Army Research laboratory, ARL-RP-192: **2007**; (c) Snyder, J.; Carter, R.; Wong, E.; Nguyen, P.; Xu, K.; Ngo, E.; Wetzel, E. Proceedings of SAMPE 2006 Symposium and Exhibition, Dallas, TX, 2006.
8. (a) O'Brien, D. J.; Baechle, D. M.; Wetzel, E. D., *J. Compos. Mater.* **2011**, *45*, 2797-2809 ; (b) Carlson, T.; Ordéus, D.; Wysocki, M.; Asp, L. E., *Compos. Sci. Technol.* **2010**, *70*, 1135-1140.
9. Simon, P.; Gogotsi, Y., *Nat. Mater.* **2008**, *7*, 845-854.
10. Kotz, R.; Carlen, M., *Electrochimica Acta* **2000**, *45*, 2483-2498.
11. Nyholm, L.; Nystrom, G.; Mihranyan, A.; Stromme, M., *Adv. Mater.* **2011**, *23*, 3751-3769.
12. Jost, K.; Perez, C. R.; McDonough, J. K.; Presser, V.; Heon, M.; Dion, G.; Gogotsi, Y., *Energy Environ. Sci.* **2011**, *4*, 5060-5067.
13. Sharma, P.; Bhatti, T. S., *Energy Convers. Manage.* **2010**, *51*, 2901-2912.
14. Zhang, L. L.; Zhao, X. S., *Chem. Soc. Rev.* **2009**, *38*, 2520-2531.
15. (a) Snyder, J. F.; E. Gienger; E. D. Wetzel; K. Xu; T. Huber; M. Kopac; P. Curtis; H. Qian; H. L. Diao; N. Shirshova; E. S. Greenhalgh; A. Bismarck; Shaffer, M. S. P. Proceedings of Army Science Conference. Orlando, FL, 2010; (b) Qian, H.; Diao, H. L.; Shirshova, N.; Greenhalgh, E. S.; Steinke, J. G. H.; Shaffer, M. S. P.; Bismarck, A., *J. Colloid Interface Sci.* **2013**, *395*, 241-248; (c) Shirshova, N.; Qian, H.; Shaffer, M. S. P.; Steinke, J. H. G.; Greenhalgh, E. S.; Curtis, P. T.; Kucernak, A.; Bismarck, A., *Composites, Part A* **2013**, *46*, 96-107.
16. (a) Qian, H.; Bismarck, A.; Greenhalgh, E. S.; Shaffer, M. S. P., *Composites, Part A* **2010**, *41*, 1107-1114; (b) Qian, H.; Bismarck, A.; Greenhalgh, E. S.; Kalinka, G.; Shaffer, M. S. P., *Chem. Mater.* **2008**, *20*, 1862-1869.
17. (a) Farmer, J. C.; Fix, D. V.; Mack, G. V.; Pekala, R. W.; Poco, J. F., *J. Electrochem. Soc.* **1996**, *143*, 159-169; (b) Pekala, R. W.; Farmer, J. C.; Alviso, C. T.; Tran, T. D.; Mayer, S. T.; Miller, J. M.; Dunn, B., *J. Non-Cryst. Solids* **1998**, *225*, 74-80; (c) Pekala, R. W., *J. Mater. Sci.* **1989**, *24*, 3221-3227.
18. (a) Lytle, J. C.; Wallace, J. M.; Sassin, M. B.; Barrow, A. J.; Long, J. W.; Dysart, J. L.; Renninger, C. H.; Saunders, M. P.; Brandell, N. L.; Rolison, D. R., *Energy Environ. Sci.* **2011**, *4*, 1913-1925; (b) Wang, J.; Glora, M.; Petricevic, R.; Saliger, R.; Proebstle, H.; Fricke, J., *J. Porous Mater.* **2001**, *8*, 159-165; (c) Schmitt, C.; Probstle, H.; Fricke, J., *J. Non-Cryst. Solids* **2001**, *285*, 277-282.
19. Williams, C.; Summerscales, J.; Grove, S., *Composites, Part A* **1996**, *27*, 517-524.
20. Kim, Y., *Power Electronics Technology Magazine* 2003, pp 34-39.
21. Kötz, R.; Carlen, M., *Electrochim. Acta* **2000**, *45*, 2483-2498.

22. ASTM-D3518, ASTM: 100 Barr Harbor Drive, West Conshohocken, PA 19428-2959, United States., 1995.
23. ASTM-D3171, ASTM: 100 Barr Harbor Drive, West Conshohocken, PA 19428-2959, United States., 2000.
24. Halama, A.; Szubzda, B.; Pasciak, G., *Electrochim. Acta* **2010**, *55*, 7501-7505.
25. Al-Muhtaseb, S. A.; Ritter, J. A., *Adv. Mater.* **2003**, *15*, 101-114.
26. Lytle, J. C.; Long, J. W.; Barrow, A. J.; Saunders, M. P.; Rolison, D. R.; Dysart, J. L. USPTO Patent Application US 2010/0189991 A1, **2010**.
27. Hull, D.; Clyne, T. W., *An Introduction to Composite Materials*. Cambridge University Press: **1981**.
28. Simon, P.; Burke, A., *Electrochem. Soc. Interface* **2008**, *Spring*, 38-43.
29. Sing, K. S. W.; Everett, D. H.; Haul, R. A. W.; Moscou, L.; Pierotti, R. A.; Rouquerol, J.; Siemieniewska, T. Pure and Applied Chemistry (IUPAC): **1985**; pp 603–619.
30. Marsh, H.; Rodriguez-reinoso, F., Characterization of activated carbon In *Activated carbon*, Marsh, H.; Rodriguez-reinoso, F., Eds. Elsevier Ltd.: Oxford, UK, **2006**; pp 143-242.
31. Zhu, Y.; Hu, H.; Li, W.; Zhang, X., *Carbon* **2007**, *45*, 160-165.
32. (a) Kalpana, D.; Omkumar, K. S.; Kumar, S. S.; Renganathan, N. G., *Electrochim. Acta* **2006**, *52*, 1309-1315; (b) Mitali, S.; Soma, D.; Monica, D., *Res. J. Chem. Sci.* **2011**, *1*, 109-113.
33. Liu, C.; Yu, Z.; Neff, D.; Zhamu, A.; Jang, B. Z., *Nano Lett.* **2010**, *10*, 4863-4868.
34. Mars, P. IEEE Technology Time Machine Symposium on Technologies Beyond 2020 (TTM), Dresden, Germany 2011; pp 1-2.
35. Snook, G. A.; Kao, P.; Best, A. S., *J. Power Sources* **2011**, *196*, 1-12.
36. Jacob, M. M. E.; Hackett, E.; Giannelis, E. P., *J. Mater. Chem.* **2003**, *13*, 1-5.
37. Kang, Y.; Cheong, K.; Noh, K.-A.; Lee, C.; Seung, D.-Y., *J. Power Sources* **2003**, *119-121*, 432-437.
38. Javid, A. Imperial College London, 2012.
39. Liang, W. J.; Chen, T. Y.; Kuo, P. L., *J. Appl. Polym. Sci.* **2004**, *92*, 1264-1270.
40. Tonurist, K.; Janes, A.; Thomberg, T.; Kurig, H.; Lust, E., *J. Electrochem. Soc.* **2009**, *156*, A334-A342.
41. Abot, J. L.; Yasmin, A.; Jacobsen, A. J.; Daniel, I. M., *Compos. Sci. Technol.* **2004**, *64*, 263-268.
42. Greenhalgh, E. S., *Failure analysis and fractography of polymer composites*. Woodhead Publishing Limited: **2009**.
43. Tong, L.; Mouritz, A. P.; Bannister, M., Introduction. In *3D Fibre Reinforced Polymer Composites*, Elsevier Science, Oxford: **2002**; pp 1-12.
44. Subramaniyan, A. K.; Sun, C. T., *Composites, Part A* **2006**, *37*, 2257-2268.
45. Qian, H.; Greenhalgh, E. S.; Shaffer, M. S. P.; Bismarck, A., *J. Mater. Chem.* **2010**, *20*, 4751-4762.
46. Hsieh, T. H.; Kinloch, A. J.; Masania, K.; Lee, J. S.; Taylor, A. C.; Sprenger, S., *J. Mater. Sci.* **2010**, *45*, 1193-1210.
47. Snyder, J. F.; Wong, E. L.; Hubbard, C. W., *J. Electrochem. Soc.* **2009**, *156*, A215-A224.
48. Park, Y.-W.; Lee, D.-S., *J. Non-Cryst. Solids* **2005**, *351*, 144-148.
49. Snyder, J. F.; Wetzel, E. D.; Watson, C. M., *Polymer* **2009**, *50*, 4906-4916.
50. (a) Lee, C. H.; Park, H. B.; Park, C. H.; Lee, S. Y.; Kim, J. Y.; McGrath, J. E.; Lee, Y. M., *J. Power Sources* **2010**, *195*, 1325-1332; (b) Souza, F. L.; Bueno, P. R.; Longo, E.; Leite, E. R., *Solid State Ionics* **2004**, *166*, 83-88.
51. Qian, H.; Kalinka, G.; Chan, K. L. A.; Kazarian, S. G.; Greenhalgh, E. S.; Bismarck, A.; Shaffer, M. S. P., *Nanoscale* **2011**, *3*, 4759-4767.







**Scheme 1.** Schematic illustration of the concept of multifunctional structural supercapacitor device based on CAG-modified structural carbon fibre fabrics as the electrodes, structural glass fabrics as the separator in a polymer-based electrolyte. Please note that the diagrams are not to scale.

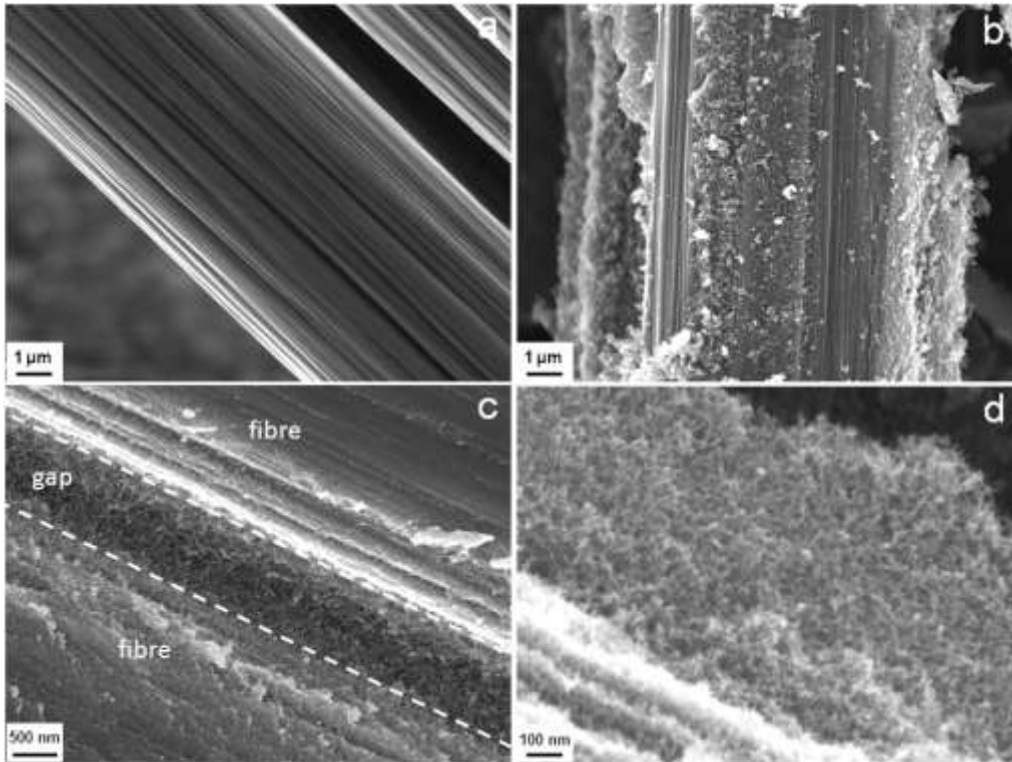


**Figure 1.** SEM images of (a) as-received carbon fibres, and (b) - (d) the fracture surfaces of CAG-embedded carbon fibre composite fabrics. CAG was successfully deposited on and around the fibres, forming a continuous matrix monolith. Note that (d) is higher magnification image of the CAG structure.

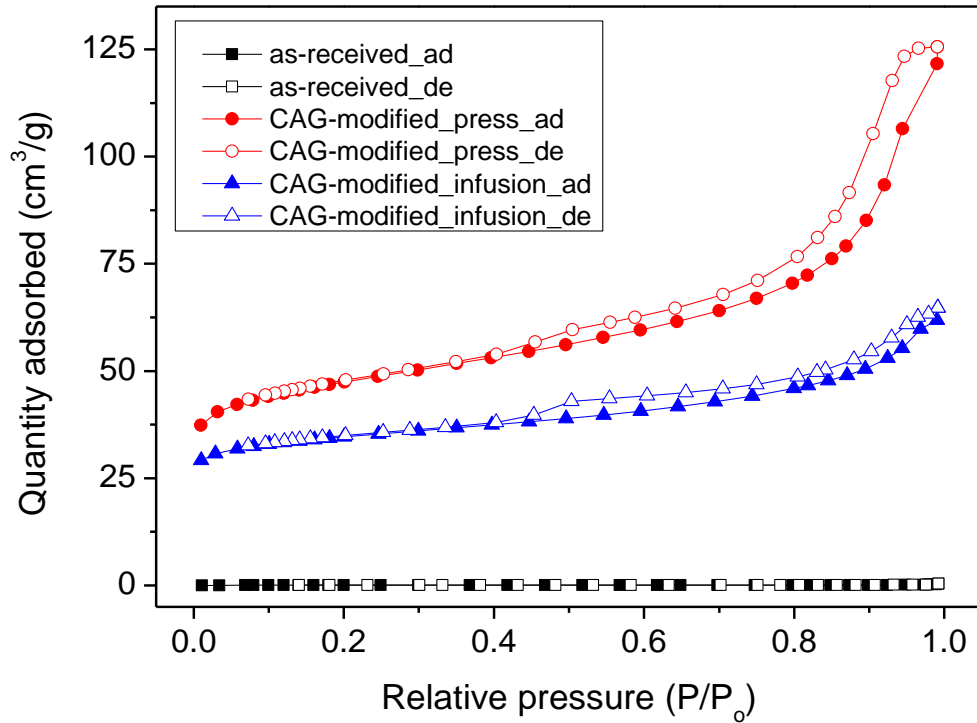


**Figure 2.** Adsorption and desorption isotherms of as-received and CAG-modified carbon fibre fabrics.

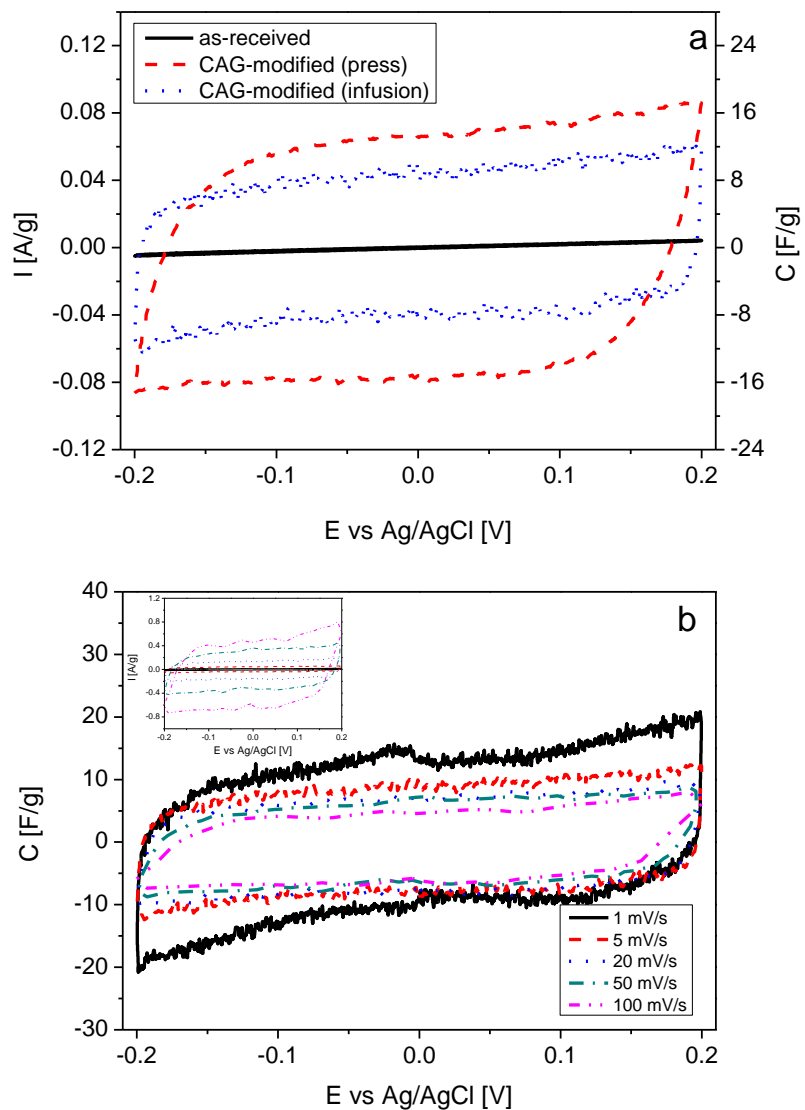


**Figure 3.** Cyclic voltammograms and capacitances (voltammograms divided by the scan rate) for (a) as-received and CAG-modified carbon fibre fabrics at 5 mV/s and (b) CAG-modified carbon fibre fabrics prepared using the infusion method at different scan rate in 3 M KCl, based on three-electrode cell testing.

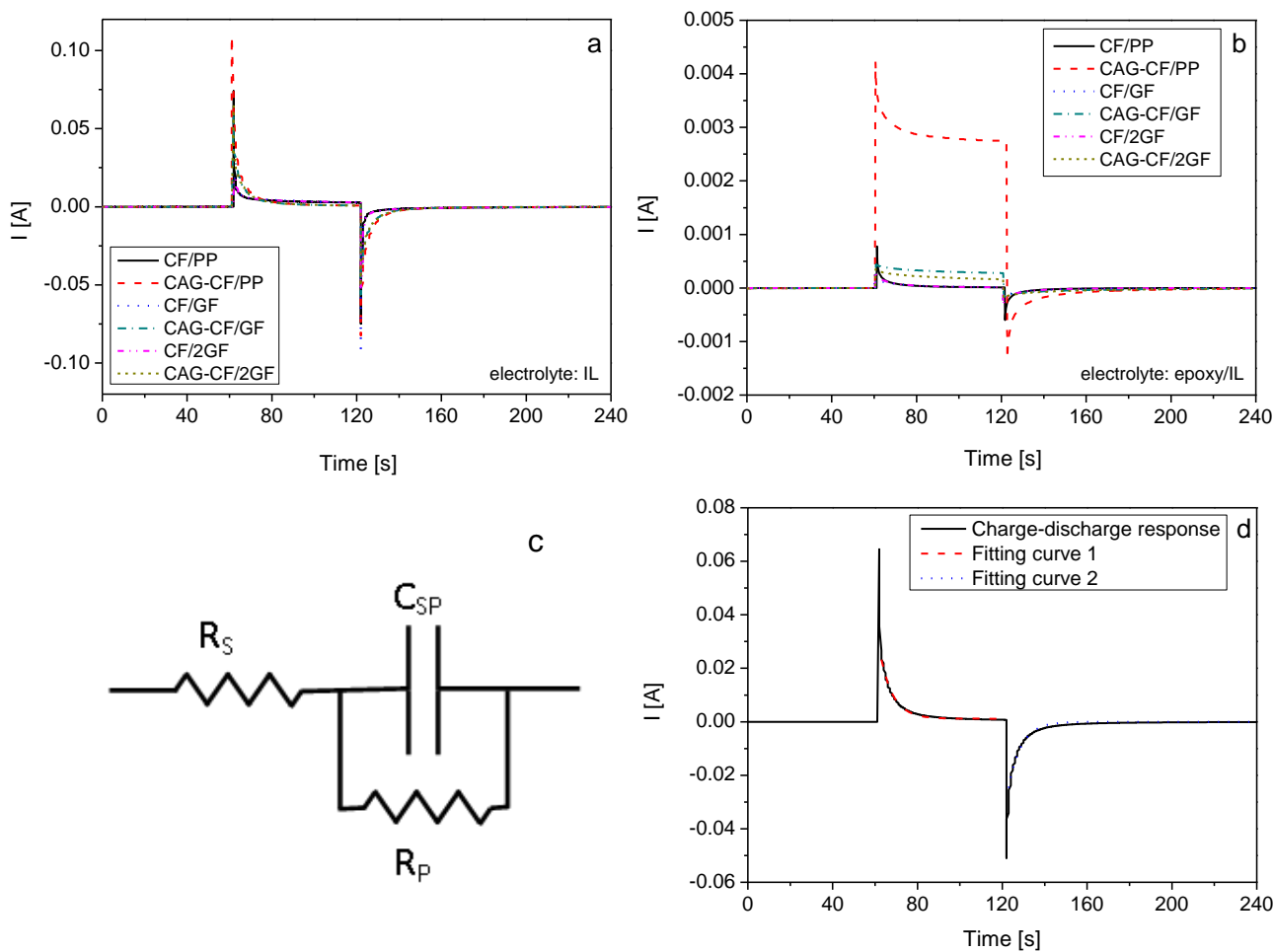


**Figure 4.** Charge-discharge response of structural supercapacitors fabricated using as-received and CAG-modified carbon fibre fabrics and different separator materials in (a) ionic liquid (currents for the CF devices were multiplied by 100) and (b) PEGDGE-based epoxy with 10 wt.% ionic liquid. (c) Equivalent circuit for the supercapacitor system.  $C_{sp}$ : capacitance;  $R_p$ : parallel resistance;  $R_s$ : equivalent series resistance. (d) An example showing the fittings to the charge and discharge transients.

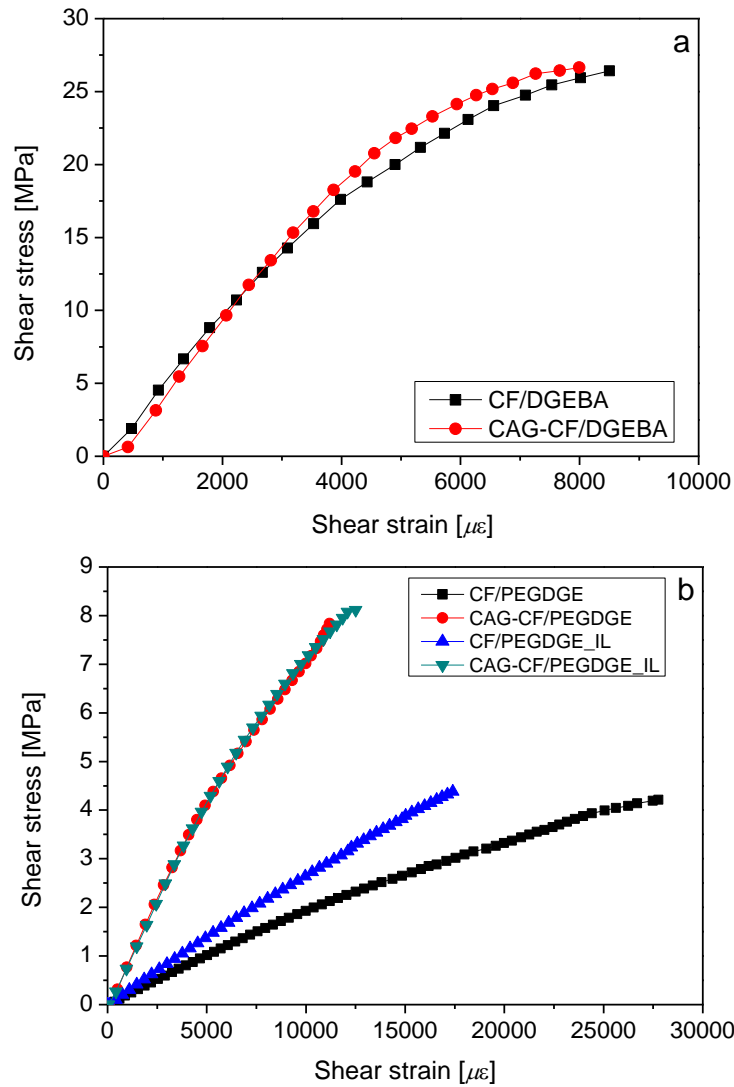


**Figure 5.** Mechanical characterisation of composite specimens fabricated using as-received and CAG-modified carbon fibre fabrics. Typical in-plane shear response of (a) DGEBA-based and (b) PEGDGE-based epoxy composites.

**Table 1.** Surface properties of as-received and CAG-modified carbon fibre fabrics and specific capacitances derived from cyclic voltammetry at a scan rate of 5 mV/s in 3M KCl using a three-electrode cell.

	CAG loading (wt.%)	BET surface area ( $\text{m}^2/\text{g}_{\text{C+CAG}}$ )	Pore volume ( $\text{cm}^3/\text{g}$ )	Pore width (nm)	Specific capacitance ( $\text{F}/\text{g}_{\text{C+CAG}}$ )	CAG-normalised surface area ( $\text{m}^2/\text{g}_{\text{CAG}}$ )	CAG-normalised capacitance ( $\text{F}/\text{g}_{\text{CAG}}$ )
As-received	n/a	$0.209 \pm 0.003$	$2.9\text{E-}4$	n/a	$0.06 \pm 0.01$	n/a	n/a
CAG-modified (pressing)	22.0	$163.1 \pm 1.8$	0.188	4.6	$14.3 \pm 0.2$	741.4	65.2
CAG-modified (infusion)	15.9	$118.0 \pm 1.6$	0.092	3.1	$8.7 \pm 0.3$	742.0	54.8
CAG-modified (infusion_scaled-up)	9.5	$80.7 \pm 0.7$	0.138	6.8	$5.9 \pm 0.4$	849.5	62.1

**Table 2.** Electrochemical properties of supercapacitors fabricated using as-received (normal) and CAG-modified (italic) carbon fibre fabrics (CAG loading around 9 wt.%) with different separator materials (PP and GF). Gravimetric (electrode mass-normalised) ( $C_g$ ), area-normalised ( $C_a$ ) and volumetric ( $C_v$ ) capacitance values were derived from charge/discharge measurements. The energy (E) and power densities (P) were calculated using the applied voltage of 0.1 V. The coefficients of variation were around 5%.

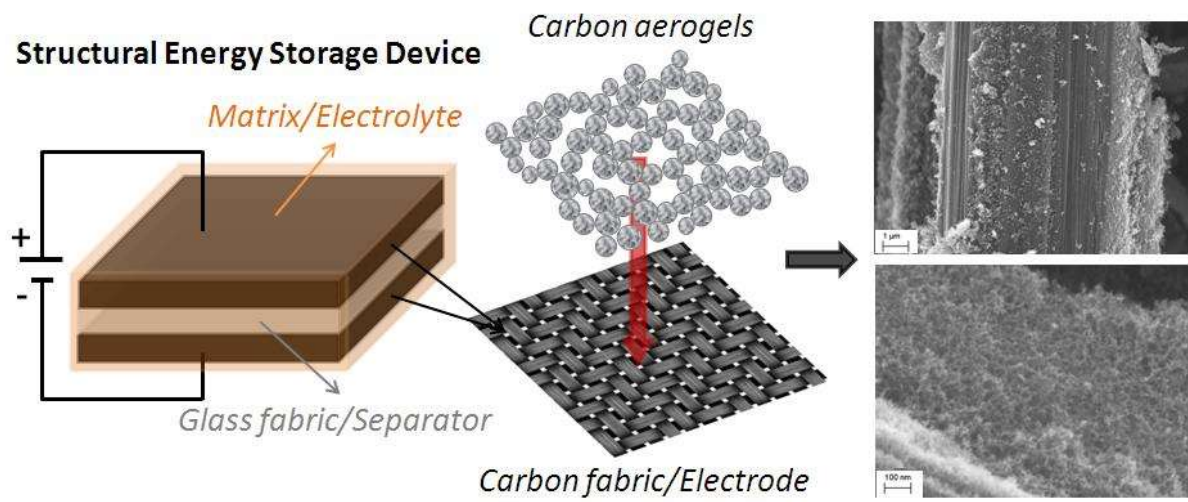
Electrode	Separator	Electrolyte	area (cm <sup>2</sup> )	$R_p$ (k $\Omega$ cm <sup>2</sup> )	$R_s$ (k $\Omega$ cm <sup>2</sup> )	$C_g$ (mF/g)	$C_a$ (mF/cm <sup>2</sup> )	$C_v$ (mF/cm <sup>3</sup> )	E ( $\mu$ Wh/kg)	P (mW/kg)
As-received	PP	IL	45.26	103.2	38.9	4.25	0.17	3.33	5.90	1.61
<i>CAG-modified</i>			<i>44.17</i>	<i>3.18</i>	<i>0.14</i>	<i>884.8</i>	<i>39.1</i>	<i>641.1</i>	<i>1230</i>	<i>420</i>
As-received	GF	IL	45.26	94.1	43.4	5.55	0.22	2.92	7.71	1.44
<i>CAG-modified</i>			<i>44.17</i>	<i>3.66</i>	<i>0.19</i>	<i>746.6</i>	<i>33.0</i>	<i>362.6</i>	<i>1040</i>	<i>300</i>
As-received	PP	PEGDGE/ 10 wt.% IL	62.05	306.3	26.3	6.52	0.26	5.11	9.06	2.38
<i>CAG-modified</i>			<i>59.50</i>	<i>0.42</i>	<i>1.72</i>	<i>602.5</i>	<i>26.6</i>	<i>436.5</i>	<i>840</i>	<i>32.8</i>
As-received	GF	PEGDGE/ 10 wt.% IL	46.08	225.7	23.7	10.7	0.43	5.62	14.8	2.64
<i>CAG-modified</i>			<i>44.73</i>	<i>14.1</i>	<i>14.7</i>	<i>71.2</i>	<i>3.15</i>	<i>34.6</i>	<i>98.9</i>	<i>3.84</i>



**Table 3.** In-plane shear test results of composites containing as-received and CAG-modified carbon fibre fabrics with different structural polymer and multifunctional polymer electrolyte matrices. Two plies of glass fabrics were used in each sample.

Reinforcement	Matrix	Shear strength (MPa)	Shear modulus (MPa)	Volume fraction of fibre reinforcement (vol.%)
As-received	DGEBA-based epoxy	$25.9 \pm 2.2$	$4380 \pm 60$	45.0
CAG-modified		$26.2 \pm 0.5$	$5050 \pm 210$	40.7
As-received	PEGDGE-based epoxy	$5.83 \pm 0.14$	$201 \pm 10$	47.2
CAG-modified		$8.88 \pm 0.12$	$911 \pm 60$	42.0
As-received	PEGDGE-based epoxy with 10 wt% IL	$5.36 \pm 0.07$	$276 \pm 14$	47.2
CAG-modified		$8.71 \pm 0.11$	$895 \pm 60$	42.0

## Table of Contents Graphic (TOC)



## Supporting Information

**Table S1.** Surface properties of different carbon fibre fabrics before and after CAG-modification using the scaled-up infusion process and specific capacitance derived from cyclic voltammetry at a scan rate of 5 mV/s in 3M KCl using a three-electrode cell.

	CAG loading (wt.%)	BET surface area (m <sup>2</sup> /g <sub>C+CAG</sub> )	Specific capacitance (F/g <sub>C+CAG</sub> )
HTA	-	0.209 ± 0.003	0.06 ± 0.01
CAG-modified HTA	9.5	80.7 ± 0.7	5.9 ± 0.4
Activated HTA	-	21.4 ± 0.1	2.6 ± 0.2
CAG-modified activated HTA	7.4	87.6 ± 0.8	6.1 ± 0.1
T300	-	0.303 ± 0.005	0.12 ± 0.01
CAG-modified T300	7.2	76.4 ± 0.6	5.0 ± 0.1

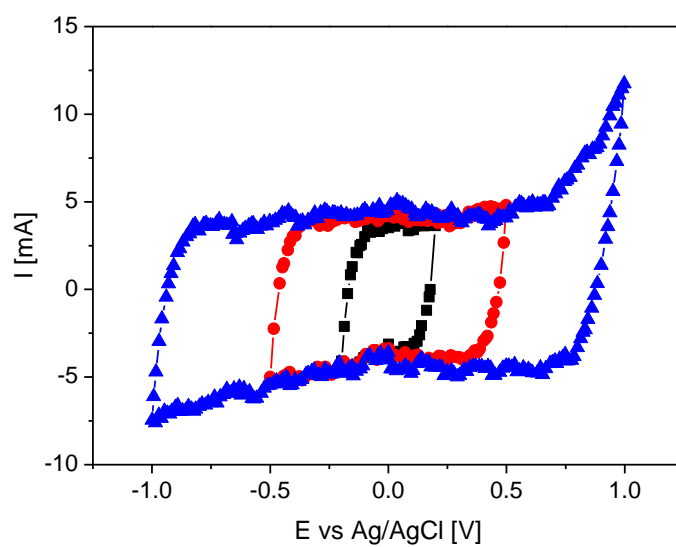


**Figure S1.** Typical cyclic voltammograms for CAG-modified carbon fibres over different potential windows at 100 mV/s, in 3 M KCl, based on three-electrode cell testing.

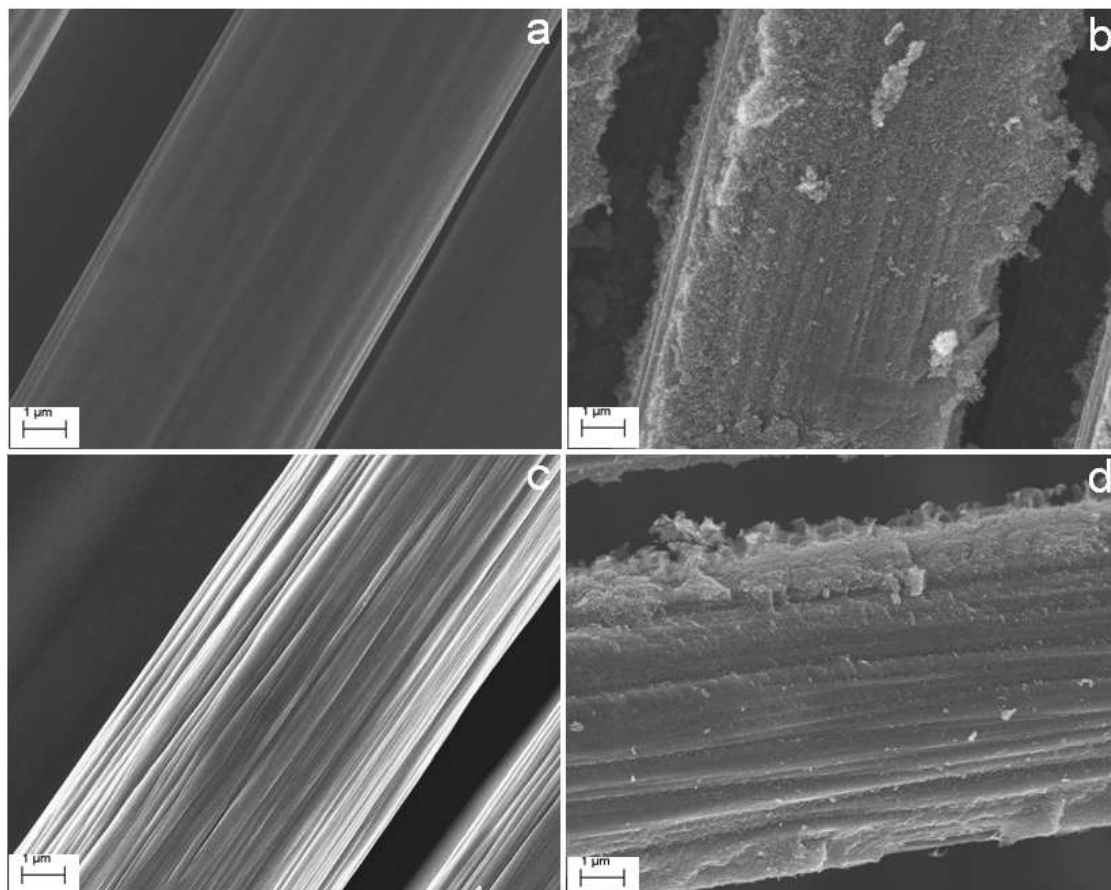


**Figure S2.** SEM images of (a) chemically-activated HTA and (c) T300 carbon fibre fabrics before (a),(c) and after (b),(d) CAG-modification.

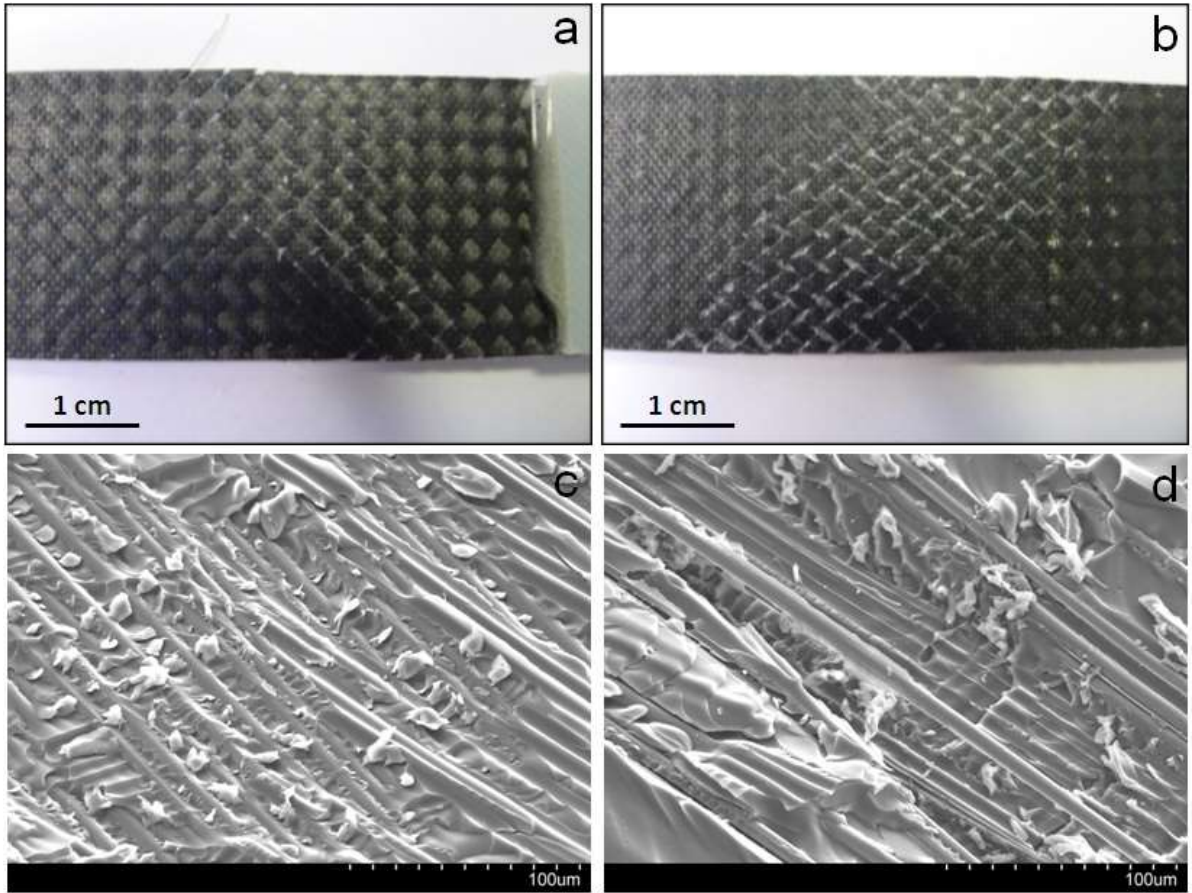


**Figure S3.** (a), (b) Photographs of failed PEGDGE-based composite specimens under in-plane shear testing. (c), (d) SEM images (taken with an Hitachi S3400 at 15 kV) of the delamination fracture surfaces. (a), (c) as-received and (b), (d) CAG-modified carbon fibre fabrics.